Development 138, 5235-5246 (2011) doi:10.1242/dev.062802

Mastermind-like 1 (MamL1) and mastermind-like 3 (MamL3) are essential for Notch signaling in vivo

Toshinao Oyama[1,*], Kenichi Harigaya[1], Nobuo Sasaki[2], Yoshiaki Okamura[2], Hiroki Kokubo[2], Yumiko Saga[2], Katsuto Hozumi[3], Akiko Suganami[4], Yutaka Tamura[4], Takahiro Nagase[5], Hisashi Koga[5], Motoi Nishimura[6], Reiko Sakamoto[7], Mitsuharu Sato[7], Nobuaki Yoshida[7] and Motoo Kitagawa[1,‡]

SUMMARY

Mastermind (Mam) is one of the elements of Notch signaling, a system that plays a pivotal role in metazoan development. Mam proteins form transcriptionally activating complexes with the intracellular domains of Notch, which are generated in response to the ligand-receptor interaction, and CSL DNA-binding proteins. In mammals, three structurally divergent Mam isoforms (MamL1, MamL2 and MamL3) have been identified. There have also been indications that Mam interacts functionally with various other transcription factors, including the p53 tumor suppressor, β-catenin and NF-κB. We have demonstrated previously that disruption of MamL1 causes partial deficiency of Notch signaling in vivo. However, MamL1-deficient mice did not recapitulate total loss of Notch signaling, suggesting that other members could compensate for the loss or that Notch signaling could proceed in the absence of Mam in certain contexts. Here, we report the generation of lines of mice null for MamL3. Although MamL3-null mice showed no apparent abnormalities, mice null for both MamL1 and MamL3 died during the early organogenic period with classic pan-Notch defects. Furthermore, expression of the lunatic fringe gene, which is strictly controlled by Notch signaling in the posterior presomitic mesoderm, was undetectable in this tissue of the double-null embryos. Neither of the single-null embryos exhibited any of these phenotypes. These various roles of the three Mam proteins could be due to their differential physical characteristics and/or their spatiotemporal distributions. These results indicate that engagement of Mam is essential for Notch signaling, and that the three Mam isoforms have distinct roles in vivo.

KEY WORDS: Notch signaling, Mastermind, Mouse

INTRODUCTION

Notch signaling is one of a small number of signaling pathways used repeatedly during metazoan development to control numerous cell fate decisions. It mediates short-range communication between cells using receptors and ligands that are present on the cell surface (Artavanis-Tsakonas et al., 1995; Bray, 2006; Greenwald, 2005; Kopan and Ilagan, 2009). In humans, abnormalities in Notch signaling have been linked to various developmental syndromes, adult-onset diseases, and cancers (Kopan and Ilagan, 2009).

The Notch genes encode single-pass transmembrane receptor molecules. On binding with ligands (Delta or Serrate/Jagged), Notch is cleaved sequentially by ADAM10 protease (Bozkulak and Weinmaster, 2009; van Tetering et al., 2009) and a tetrameric γ-secretase complex at a luminal juxtamembrane site and at an intramembrane site, respectively, releasing the intracellular (IC) domain from the membrane. Acting as a second messenger in the signaling pathway, the NotchIC domain is transported to the nucleus and participates in transcriptional activation through association with promoter elements via the CBF-1, Su(H) and Lag-1 (CSL) [recombination signal sequence-binding protein J (RBP-J) in mammals] DNA-binding proteins. In mammals, the Hes and Hesr (also known as Hey, Herp, Hrt, CHF or gridlock) families are among the primary target genes of the Notch signaling pathway (Bray, 2006; Kopan and Ilagan, 2009). Mice deficient in one of several essential elements in this signaling pathway die in midgestation with distinctive defects: defective vascular remodeling, aberrant somitogenesis and enhanced neurogenesis (Barsi et al., 2005; Chen et al., 2009; de la Pompa et al., 1997; Donoviel et al., 1999; Hartmann et al., 2002; Herreman et al., 1999; Koo et al., 2005; Li et al., 2003; Oka et al., 1995; Serneels et al., 2005; Shi and Stanley, 2003). These are considered to be the pan-Notch phenotypes.

Mastermind (Mam) is one of the components of Notch signaling. Genetic analyses in *Drosophila* and *Caenorhabditis elegans* have implied that Mam is an essential positive regulator of this pathway in these species, which possess a single Mam gene in their genomes (Artavanis-Tsakonas et al., 1995; Greenwald, 2005). We and others have identified a family of Mam genes/proteins in humans, consisting of three members, MAML1 (for Mam-like 1; also known as Mam-1), MAML2 (Mam-3) and MAML3 (Mam-2), and have elucidated their biochemical mechanisms of action (Kitagawa et al., 2001; Lin et al., 2002; Wu et al., 2000; Wu et al., 2002). All the Mam proteins bind to and stabilize the DNA-binding complex of the NotchIC and CSL proteins in the nucleus. Neither the single NotchIC nor the CSL proteins are able to associate stably

[1]Department of Molecular and Tumor Pathology, Chiba University Graduate School of Medicine, 1-8-1 Inohana, Chuo-ku, Chiba 260-8670, Japan. [2]Division of Mammalian Development, National Institute of Genetics, 1111 Yata, Mishima, Shizuoka 411-8540, Japan. [3]Department of Immunology, Tokai University School of Medicine, Bohseidai, Isehara, Kanagawa 259-1193, Japan. [4]Department of Bioinformatics, Chiba University Graduate School of Medicine, 1-8-1 Inohana, Chuo-ku, Chiba 260-8670, Japan. [5]Kazusa DNA Research Institute, 2-6-7 Kazusa-Kamatari, Kisarazu, Chiba 292-0818, Japan. [6]Department of Molecular Diagnosis, Chiba University Graduate School of Medicine, Inohana 1-8-1, Chuo-ku, Chiba 260-8670, Japan. [7]Institute of Medical Science, The University of Tokyo, 4-6-1 Shirokane-dai, Minato-ku, Tokyo 108-8639, Japan.

*Present address: Memorial Sloan-Kettering Cancer Center, New York, NY 10065, USA
‡Author for correspondence (kitagawa@faculty.chiba-u.jp)

Accepted 24 September 2011

with Mam proteins. Concurrently with this ternary complex formation, the activation of transcription from target promoters is potentiated. The three human Mam proteins show remarkable similarities in their functions in vitro, although having an unusual structural diversity. For complex formation, the three mammalian Mam proteins exhibit little preference among the four mammalian Notch proteins. Furthermore, all the Mam proteins can augment the transcription evoked by all the NotchIC domains to comparable degrees. The MAML1 and MAML3 proteins are the most highly related among the family, with 30% identity in the primary structure. The crystal structures of the core parts of the Mam-NotchIC-CSL ternary complex bound to DNA have been described (Nam et al., 2006; Wilson and Kovall, 2006). These structures are consistent with the model that we proposed.

This transcriptionally active complex appears to be a point of regulation induced by other signaling cues. The formation of this complex is negatively regulated by phosphorylation of Notch by Nemo-like kinase, an evolutionarily conserved, multifunctional protein kinase (Ishitani et al., 2010). The multifunctional transcriptional repressor Bcl6 competes with Mam for association with Notch and CSL to repress selected target genes (Sakano et al., 2010). During somitogenesis, destabilization of Mam by Mesp2 to repress Notch signaling has been shown to be an essential process (Sasaki et al., 2011). Various covalent modifications of Mam itself have also been reported to regulate the signaling (Lindberg et al., 2010). A stapled α-helical peptide derived from the Notch-binding domain of MAML1 strongly inhibits Notch signaling, both in vitro and in vivo (Moellering et al., 2009). Furthermore, there have been indications that MamL1 interacts functionally with various other transcription factors, namely Mef2c, the p53 tumor suppressor (Trp53 – Mouse Genome Informatics), β-catenin, and NF-κB (Alves-Guerra et al., 2007; Jin et al., 2010; Shen et al., 2006; Zhao et al., 2007).

We and others have previously shown that MamL1 deficiency in mice results in partial disruption of the Notch signal-dependent developmental steps in lymphopoiesis, especially those steps that require relatively strong signaling (Oyama et al., 2007; Wu et al., 2007). We have also reported that MamL1 deficiency in primary cultured fibroblasts results in reduced activation of a target promoter upon expression of an exogenous NotchIC domain (Oyama et al., 2007). These results indicate that Notch signaling is partially dependent on MamL1. However, the in vivo functions of the other Mam proteins remain elusive. Furthermore, it is also unknown whether Mam is essential for mammalian Notch signaling or whether it is an auxiliary component used to achieve maximum signal strength.

Here, we describe the generation of MamL3-deficient mice. Although MamL3-null mice have no apparent abnormalities, including the Notch signal-dependent steps in lymphocyte development, embryos null for both MamL1 and MamL3 exhibit the distinctive phenotypes of the pan-Notch defects and reduced expression of Notch target genes. Furthermore, expression of a gene under strict control of Notch signaling during a developmental process is undetectable in the double-null embryos. Thus, Mam is an essential component of Notch signaling in mammals and the two of the three isoforms play a major role during the organogenic period in mice.

MATERIALS AND METHODS

MamL3- and MamL1-deficient mice

A genomic clone containing *MamL3* was isolated by screening a genomic library generated from a mouse of the 129 strain with a cDNA encoding murine *MamL3* (IMAGE clone 3709010) as a probe. A targeting vector was then constructed in pMC1NeoPolyA (Agilent Technologies, Santa Clara, CA, USA). A diphtheria toxin A gene cassette was ligated at the 3′ end of the targeting vector. The vector was linearized at the 5′ end and then introduced into E14-1 embryonic stem (ES) cells (129P2/Ola strain) by electroporation. After selection in a medium containing G418 (400 μg/ml; Invitrogen, Carlsbad, CA, USA), clones harboring a targeted allele were identified by Southern blotting using standard procedures. The targeting frequency was ~2%. ES cells with the targeted allele were injected into blastocysts of the C57BL/6 strain (CLEA Japan, Tokyo, Japan). Chimeric males were mated with females of the C57BL/6 strain to obtain heterozygous mice. All animals were genotyped by either Southern blotting or PCR. Germline transmission was obtained from two of the clones. Results obtained with mice from these two lines were indistinguishable. MamL1-deficient mice were as described (Oyama et al., 2007). The mice were maintained by backcrossing to the C57BL/6 strain. All mice were kept under specific pathogen-free conditions. All the protocols for animal experiments were approved by the Committee of Animal Experiments, Chiba University.

Cell culture and luciferase assay

Primary cultured embryonic fibroblasts (EFs) were prepared from 14.5 days post-coitum (dpc) embryos and cultured in Dulbecco's modified Eagle's medium (DMEM; Nissui Pharmaceutical, Tokyo, Japan) supplemented with 10% fetal bovine serum (FBS). 293T cells were cultured in DMEM supplemented with 10% FBS. EFs seeded on 12-well plates were transfected with pEF-BOSneo with or without Notch1IC, Notch2IC, Notch3IC, or Notch4IC (Lin et al., 2002), pTP1-luc (Minoguchi et al., 1997) and *Renilla* luciferase internal control plasmid (pRL-CMV; Promega, Madison, WI, USA) using FuGENE 6 Transfection Reagent (Roche, Basel, Switzerland). Two days after the transfection, the firefly and *Renilla* luciferase activities were determined using a Dual Luciferase Assay Kit (Promega) and a TD20/20 dual luminometer (Turner Designs, Sunnyvale, CA, USA). Firefly luciferase activities were normalized to the *Renilla* luciferase control activities. 293T cells were transfected with FuGENE 6.

Western blotting

Western blotting was performed as described previously (Oyama et al., 2007). $B220^+$ splenocytes were sorted from splenic cells of an 8-week-old female C57BL/6 mouse using fluorescein isothiocyanate (FITC)-anti-mouse/human B220 antibody (CD45R; eBioscience, San Diego, CA, USA), anti-FITC antibody-conjugated paramagnetic MicroBeads (Miltenyi Biotec, Bergisch Gladbach, Germany), and an autoMACS separator (Miltenyi Biotec). In the fraction that contained protein extract, 97.1% of the cells were positive for B220. The antibodies used for blotting were: anti-MAML1 (Lin et al., 2002), anti-MAML3 (A300-684A; Bethyl Laboratories) and anti-MAML2 (A300-682A; Bethyl Laboratories) in Fig. 1D and Fig. 9B; anti-MAML1 (A300-673A; Bethyl Laboratories, Montgomery, TX, USA) and anti-MAML2 (#4618; Cell Signaling Technology, Danvers, MA, USA) in Fig. 9A,C,D; anti-NOTCH1 (sc-6014; Santa Cruz Biotechnology, Santa Cruz, CA, USA); anti-NOTCH2 (sc-5545; Santa Cruz Biotechnology); anti-Hes1 (a gift from T. Sudo, Toray Pharmaceutical Research Laboratories, Kamakura, Japan); and anti-Myc-Tag (047-3; Medical & Biological Laboratories, Nagoya, Japan).

Real-time PCR

Isolation of total RNA and real-time PCR were performed as described previously (Oyama et al., 2007). The expression of glyceraldehyde-3-phosphate dehydrogenase was used as an internal control. See supplementary material Table S1 for primer sequences.

Flow cytometry

The reagents used for analyzing the development of thymocytes and splenocytes were as follows: FITC-conjugated-CD21, PerCp-Cy5.5-CD4, PerCp-Cy5.5-CD8 and phycoerythrin (PE)-DX5 were purchased from BD Biosciences (Franklin Lakes, NJ, USA); PE-CD23, allophycocyanin (APC)-B220, FITC-CD44, PE-CD25, FITC-TCRαβ, PE-TCRγδ, APC-CD8 and FITC-Thy-1.2 were purchased from eBioscience. After staining, the cells were analyzed with a FACSCalibur (BD Biosciences).

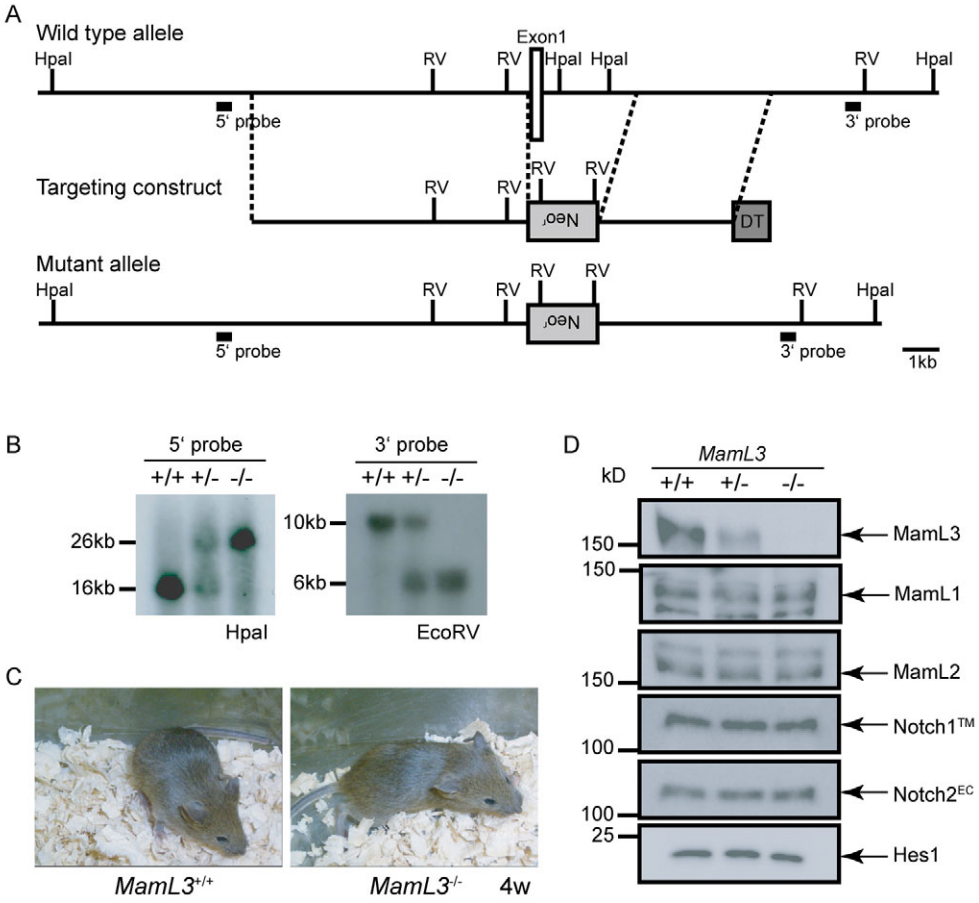

Fig. 1. Targeted disruption of the murine *MamL3* gene. (**A**) Schematics of the wild-type *MamL3* allele around exon 1, the targeting construct and the mutant allele. Southern blotting probes are indicated. DT, diphtheria toxin A gene; Neo^r, neomycin resistance gene; RV, EcoRV. (**B**) Southern blot analysis of DNAs isolated from wild-type (+/+), heterozygous (+/–) and homozygous (–/–) mice. The restriction enzymes and probes used are indicated. The sizes of the hybridizing fragments are also indicated. (**C**) A 4-week-old *MamL3*$^{-/-}$ mouse and its littermate. (**D**) Western blotting of whole cell extracts of primary cultured EFs. The genotypes of the cells, the mobility of the size markers and the identity of the bands are shown. TM, transmembrane subunit; EC, extracellular subunit.

Whole-mount immunostaining and in situ hybridization

Embryos for immunostaining were fixed in 4% paraformaldehyde in phosphate-buffered saline for 30 minutes at 4°C and incubated with an antibody for platelet-endothelial cell adhesion molecule 1 (Pecam1) (557355; BD Biosciences) overnight at 4°C. A Vectastain Elite ABC Kit (Vector Laboratories, Burlingame, CA, USA) was used for chromogenic development. Whole-mount RNA in situ hybridization was performed as described (Saga et al., 1996) with probes for *Uncx4.1* (*Uncx* – Mouse Genome Informatics) (Mansouri et al., 1997), *Mash1* (*Ascl1* – Mouse Genome Informatics) (Hatakeyama et al., 2004), delta-like1 (*Dll1*) (Hatakeyama et al., 2004) and lunatic fringe (*Lfng*) (Evrard et al., 1998).

Molecular modeling and calculation of binding energy

The three-dimensional structures of murine Notch/RBP-J/DNA with either one of murine MamL1, MamL2 or MamL3 were constructed using the Molecular Operating Environment (MOE; version 2008; CCG, Montreal, Canada) based on the Brookhaven Protein Databank 2QC9 for NOTCH1, 3BRG for RBP-J (CSL), and 2F8X for MAML1. Molecular mechanics calculations for these complexes were performed to prepare the initial structures for the molecular dynamics (MD) simulations using the Amber99 force field in MOE. MD simulations for these complexes were performed using the program AMBER 9 (http://ambermd.org/) with the AMBER force field and the modified TIP3P every 2 fseconds. To calculate the interaction energies and electrostatic complementarities, we employed MOE and MolFeat-EC (FiatLux, Tokyo, Japan) as previously described (Tonooka et al., 2009) with some modifications. The three-dimensional structures of the complexes were displayed using MolFeat (Ver. 4; FiatLux). All figures from the MD simulations of these complexes were produced using VMD (http://www.ks.uiuc.edu/Research/vmd/).

Plasmids

cDNAs with the full coding regions of murine *MamL1* (mKIAA0200) (Okazaki et al., 2003) and murine *MamL3* (Nishimura et al., 2004) have been described previously. The GenBank accession numbers for the *MamL1* and *MamL3* cDNAs are AK129088 and AB553633, respectively. A Myc-tag epitope derived from pCMV-Tag3 (Stratagene, La Jolla, CA, USA) was fused in-frame to the N-terminus of the coding region of both of the cDNAs. The coding region of the tagged proteins was cloned into pEF-BOS (Mizushima and Nagata, 1990).

RESULTS

Targeting of the *MamL3* gene

The gene encoding *MamL3* was disrupted in murine ES cells by inserting the neomycin selection cassette to replace exon 1, which encodes the initiator methionine codon and the basic domain that is essential for the association with Notch and RBP-J (Lin et al., 2002) (Fig. 1A). Clones harboring the targeted allele were used to generate chimeric mice, which were mated with C57BL/6 mice. Mice

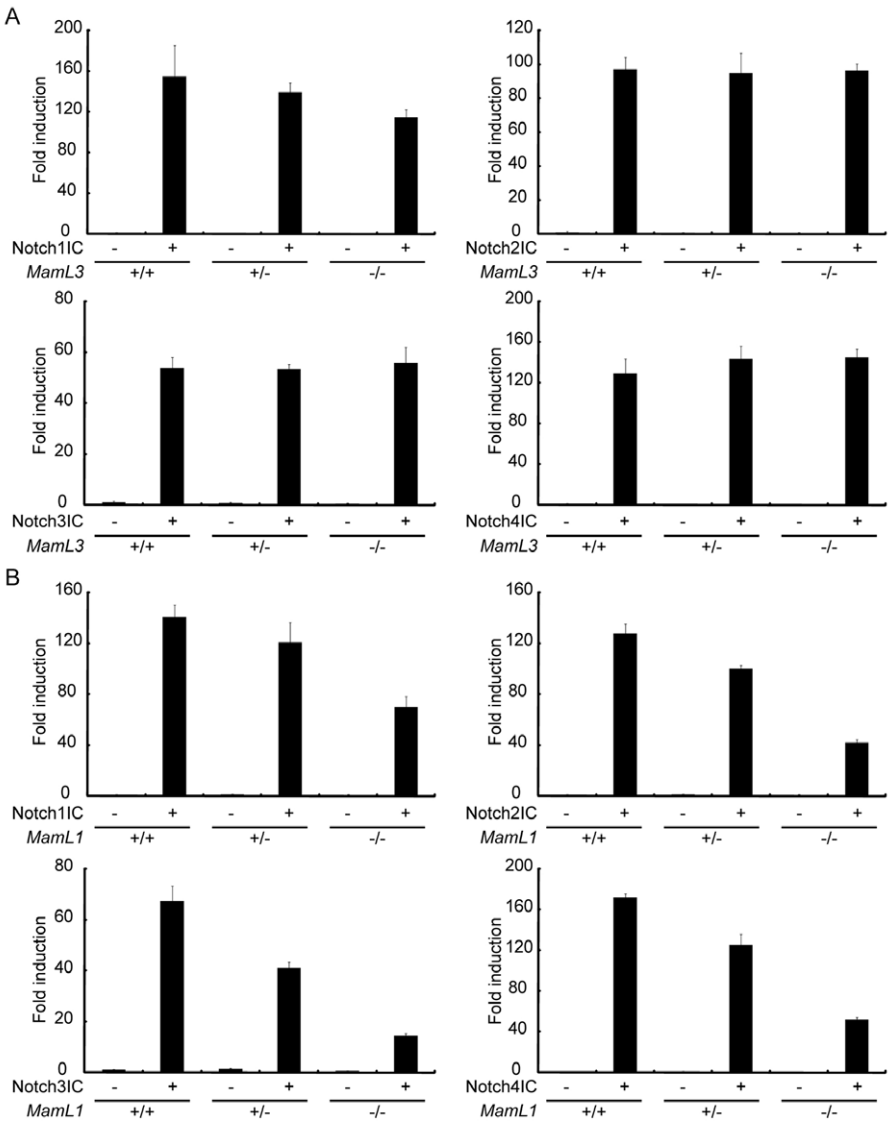

Fig. 2. Differential roles of MamL3 and MamL1 on transactivation induced by the expression of NotchICs in EFs. Luciferase assay with EFs obtained from (**A**) *MamL3*$^{-/-}$ or (**B**) *MamL1*$^{-/-}$ embryos and their respective littermates. The cells were transfected with a reporter, an internal control for transfection and expression vectors for the indicated proteins (+) or empty vectors (–). The *y*-axis represents the mean normalized luciferase activity relative to the mean activity of the wild-type cells transfected with empty vector controls. Error bars indicate s.d. (*n*=3).

heterozygous for the targeted allele appeared normal and were fertile. When the heterozygous mice were intercrossed, wild-type, heterozygous and homozygous offspring were born in the expected Mendelian ratios (Fig. 1B). In contrast to the mice deficient in MamL1 that exhibited growth retardation and succumbed before weaning (Oyama et al., 2007), *MamL3*$^{-/-}$ mice were viable, looked healthy and were fertile (Fig. 1C). Thus far, there were no obvious abnormalities in *MamL3*$^{-/-}$ mice, including those related to the deficiencies of Mef2c, p53, β-catenin and NF-κB.

As revealed by western blotting analysis of EFs, the MamL3 protein was undetectable in homozygous cells whereas it was expressed in wild-type cells (Fig. 1D). The expression of MamL3 in the heterozygous cells was intermediate. As the antibody was raised against the C-terminal portion of the protein, and no specific band with aberrant mobility was detected in the homozygous cells (T.O. and M.K., unpublished), there was no evidence for generation of truncated proteins by the targeted allele. The expression of MamL1, MamL2, Notch1, Notch2 and Hes1 was not affected by the disruption of MamL3 (Fig. 1D). When we quantitated the mRNA levels of *MamL1*, *MamL2*, *MamL3* and *Hes1* in fibroblasts by real-time PCR (supplementary material Fig. S1), the results were consistent with those obtained by the western blotting shown in Fig. 1D. As the primers for *MamL3* were directed against a portion of exon 5, there again was no evidence for the generation of a truncated gene product. These results thus indicate that MamL3 was inactivated by the gene targeting.

To evaluate the contribution of MamL3 to Notch signaling, a reporter assay was performed with the EFs. Regardless of the MamL3 genotype, expression of any of the four paralogs of NotchIC activated a reporter for intracellular Notch signaling to a similar degree (Fig. 2A). In contrast to these results, and consistent with a previous publication (Oyama et al., 2007), activation of the reporter by the NotchICs in MamL1-null EFs was markedly reduced compared with that in the wild-type EFs. Interestingly, the activation in the heterozygous EFs was intermediate between the wild-type and the null EFs, especially for Notch2IC, Notch3IC or Notch4IC, indicating haploinsufficiency of the *MamL1* gene (Fig. 2B).

MamL1 deficiency causes disruption of splenic marginal zone B (MZB) cell formation and partial impairment through the CD4^{-}CD8^{-} double-negative stages in thymocyte development (Oyama et al., 2007). However, the number of splenocytes and the proportion of MZB cells among the B220^{+} B cells in the spleen were equivalent between the MamL3-deficient mice and the wild-type littermate mice (Fig. 3A). Furthermore, we found no

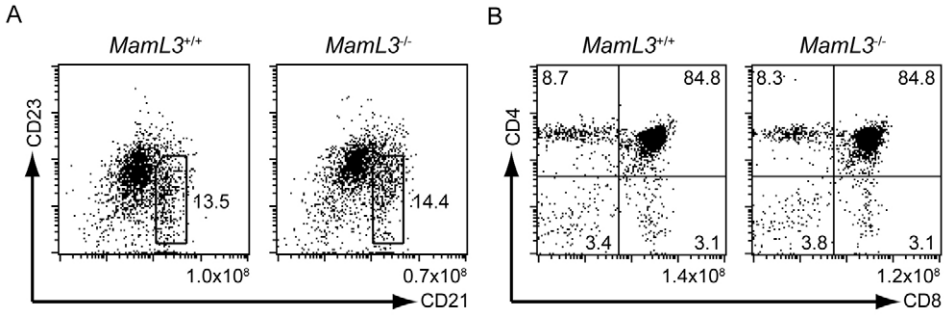

Fig. 3. Normal lymphocyte development in *MamL3*$^{-/-}$ mice. (**A**) FACS analysis of splenic B cells from 8-week-old mice. The profiles were gated on B220^{+} cells. Numbers of splenocytes are also shown. (**B**) FACS analysis of thymocytes from 8-week-old mice. Numbers of thymocytes are also shown. The numbers in the profiles represent the percentages of cells in the indicated areas.

significant differences between the MamL3-deficient and the wild-type mice in the number of thymocytes, in the CD4 and CD8 phenotypes (Fig. 3B) and in the various phenotypes of the CD4^{-}CD8^{-} double-negative fraction of the cells (supplementary material Fig. S2). Thus, we found no apparent phenotype associated with deficiency or decrease of Notch signaling in the MamL3-null mice.

Mice lacking both MamL1 and MamL3 die in midgestation with distinctive pan-Notch defects

One explanation for the lack of phenotypes in the MamL3-deficient mice is that other member(s) of the Mam family are compensating for the loss of MamL3. To examine this possibility, we intercrossed the MamL3-deficient and the MamL1-deficient strains (Oyama et al., 2007). The *MamL1*$^{+/-}$;*MamL3*$^{+/-}$ double heterozygous animals exhibited no apparent phenotype. However, analysis of the offspring from the intercrosses of these double heterozygotes demonstrated that loss of both *MamL1* and *MamL3* resulted in lethality during midgestation (Table 1). In mice with a mixed 129P2/Ola and C57BL/6 background, the doubly deficient embryos survived up to 12.5 dpc. However, when the intercrosses were performed with those backcrossed to C57BL/6 for more than five generations, the presence of double-deficient embryos obeyed Mendel's law only until 8.5-9.5 dpc. The *MamL1*$^{-/-}$;*MamL3*$^{-/-}$ double-null embryos were significantly under-represented at 10.5 dpc on this background (Table 1).

At 9.5 to 10.5 dpc, the yolk sacs of the double-null embryos had a rough texture compared with those of their littermates, and their vessels were hardly visible (Fig. 4A,B). Most double-null embryos were smaller than the littermate controls (Fig. 4C,D). The double-deficient embryos had a single branchial arch, whereas the control embryos carried at least two branchial arches (Fig. 4C,D, arrowheads). Furthermore, the double-null embryos often demonstrated enlarged pericardial sacs and poorly folded hearts (Fig. 4D, arrow). Staining for the endothelial marker Pecam1 revealed that the blood vessels were present in the embryos of the double-null mutants, but the structure was more primitive and less finely branched in the head region compared with that of the littermates (Fig. 4E-H). These phenotypes of the double-null embryos resembled those observed in the array of mutants that are deficient in Notch signaling (Barsi et al., 2005; Chen et al., 2009; Donoviel et al., 1999; Hartmann et al., 2002; Herreman et al., 1999; Koo et al., 2005; Li et al., 2003; Roca and Adams, 2007; Serneels et al., 2005; Shi and Stanley, 2003).

Defective somitogenesis is another characteristic phenotype of mutants that are deficient in Notch signaling (Dequeant and Pourquie, 2008; Oka et al., 1995). As shown in Fig. 5, the double heterozygous or either of the single-null mutants at 9.5 dpc showed iterated domains of expression of *Uncx4.1*, a homeobox gene expressed in the posterior half of mature somites. By contrast, *Uncx4.1* was undetectable in the segmental plates of the double-null embryos (Fig. 5D). This phenotype resembled those of the mutants deficient in the essential elements of the Notch signaling pathway (Koo et al., 2005; Shi and Stanley, 2003), consistent with the notion that Notch signaling is deficient during somite development in the absence of both MamL1 and MamL3.

Another distinctive phenotype caused by deficient Notch signaling is accelerated neurogenesis because of a lack of lateral inhibition in the nervous system (de la Pompa et al., 1997; Kageyama et al., 2008). We first analyzed the expression of five relevant markers by real-time PCR on total RNA isolated from whole embryos at 9.5 dpc. As shown in Fig. 6A, expression of the neuronal marker *Map2* (*Mtap2* – Mouse Genome Informatics), the proneural transcription factors *Mash1* and *Math3* (*Neurod4* –

Table 1. Lethality of double-null mice prior to 10.5 dpc

	Genotype (*MamL1*;*MamL3*)									
Stage	+/+;+/+	+/+;+/–	+/+;–/–	+/–;+/+	+/–;+/–	+/–;–/–	–/–;+/+	–/–;+/–	–/–;–/–	Total
8.5 dpc	6 (8.1%)	7 (9.5%)	5 (6.8%)	16 (22.2%)	21 (28.4%)	9 (12.1%)	2 (2.7%)	3 (4.0%)	5 (6.8%)	74 (100%)
9.5 dpc	21 (9.5%)	31 (14.1%)	20 (9.1%)	27 (12.3%)	51 (23.2%)	21 (9.5%)	17 (7.7%)	24 (10.9%)	8 (3.6%)	220 (100%)
10.5 dpc	3 (4.9%)	6 (9.8%)	4 (6.6%)	15 (24.6%)	12 (19.7%)	6 (9.8%)	6 (9.8%)	8 (13.1%)	1 (1.6%)	61 (100%)
11.5 dpc	1 (4.0%)	4 (16.0%)	3 (12.0%)	4 (16.0%)	6 (24.0%)	2 (8.0%)	2 (8.0%)	3 (12.0%)	0 (0%)	25 (100%)
P1	8 (6.3%)	22 (17.2%)	13 (10.2%)	30 (23.4%)	43 (33.6%)	12 (9.4%)	0 (0%)	0 (0%)	0 (0%)	128 (100%)
Expected rate	6.25%	12.5%	6.25%	12.5%	25.0%	12.5%	6.25%	12.5%	6.25%	100%

Numbers of progeny obtained from intercrosses of *MamL1*$^{+/-}$;*MamL3*$^{+/-}$ mice backcrossed to the C57BL/6 strain for more than five generations are shown. The percentages of the total numbers of embryos at each stage are shown in parentheses. The expected percentages based on Mendelian distribution are also shown. P, postnatal day.

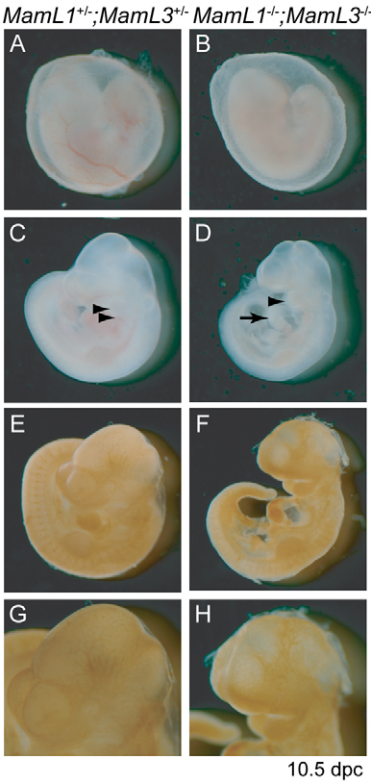

Fig. 4. Morphological abnormalities in *MamL1*$^{-/-}$;*MamL3*$^{-/-}$ double-null mutant mice at 10.5 dpc. Double-null embryos (B,D,F,H) and control littermates (A,C,E,G) are shown. (**A**,**B**) Yolk sacs at 10.5 dpc. (**C**,**D**) Embryos at 10.5 dpc. Arrowheads show the branchial arches. The arrow shows the heart of a double-null mutant. (**E**,**F**) Whole-mount immunostaining for Pecam1 of the embryos shown in C and D. (**G**,**H**) Magnified views of the head regions in E and F, respectively.

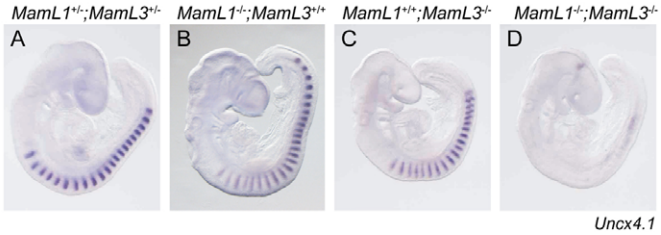

Fig. 5. Defective somite differentiation in *MamL1*$^{-/-}$;*MamL3*$^{-/-}$ double-null mutant mice. (**A-D**) Whole-mount in situ hybridization for *Uncx4.1* of embryos at 9.5 dpc. The genotypes of each embryo are indicated. Somite counts of each embryo as judged by the numbers of *Uncx4.1*-positive domains are: A, 21; B, 25; C, 20; D, 0. Note that the embryos shown in A, C, and D are littermates. A wild-type littermate of the embryo shown in B had 23 somites (T.O., N.S. and M.K., unpublished).

Mouse Genome Informatics), expression of which is repressed by Hes (Hatakeyama et al., 2004), and *Dll1*, which is a target gene of the proneural transcription factors in the nervous tissue, was elevated in the double-null mutants compared with the control littermates. By contrast, both the single-null mutants expressed these mRNAs at levels comparable to those in the control littermates (Fig. 6A).

We then assessed the phenotype by in situ hybridization. Expression of *Mash1* was upregulated in the nervous tissue of the double-null (Fig. 6E) but not of either of the single-null (Fig. 6C,D) embryos, compared with the controls (Fig. 6B). Furthermore, *Dll1* was ectopically expressed in the neural tube and was upregulated in the forebrain and hindbrain in the double-null (Fig. 6I) but not in either of the single-null (Fig. 6G,H) embryos, compared with the controls (Fig. 6F). These results indicated that accelerated neurogenesis was present in the double-null but not in either of the single-null mice. In addition, the metameric expression of *Dll1* that was observed in the control and the single-null embryos was hardly visible in the double-null embryos (Fig. 6F-I). These results are consistent with a deficiency of somitogenesis in the double-null embryos, as *Dll1* is expressed in somites (Hrabe de Angelis et al., 1997).

Overall, these analyses revealed that mice doubly deficient for both MamL1 and MamL3 exhibited all the major phenotypes found in mutants that are null for Notch signaling. Thus, it can be considered that MamL1 and MamL3 are essential core elements of the Notch signaling pathway. By contrast, as single deficiency of MamL1 or MamL3 induced none of these phenotypes, we suggest that MamL1 and MamL3 are genetically equivalent and perform redundant roles in these developmental processes.

Expression of Notch target genes is reduced in mice lacking both MamL1 and MamL3

We also analyzed the expression of an assortment of Notch signaling target genes in the total RNA isolated from the embryos. Expression of *Hes5*, *Hesr1* (*Hey1* – Mouse Genome Informatics) and *Hesr3* (*Heyl* – Mouse Genome Informatics) was reduced in the double-null mutants but not in either of the single-null mutants compared with the control littermates at 9.5 dpc (Fig. 7A). These results provide further evidence that MamL1 and MamL3 are essential for Notch signaling during development. Interestingly, expression of *Hes1* and *Hesr2* was unaffected even in the double-null mutants. The pattern of changes in *Hes1* and *Hes5* expression was similar to those observed in the mutants for RBP-J or Notch1, although the degree of reduction of Hes5 expression might be more modest compared with the mutant for RBP-J (de la Pompa et al., 1997). These results might thus be consistent with the notion that MamL1 and MamL3 function in the same pathway as RBP-J and Notch1. Expression of *Hes1*, *Hes5* and *Hesr* has been shown to be sustained not only by Notch signaling but also by other signaling cues (Itoh et al., 2004; Nakashima et al., 2001; Sanalkumar et al., 2010; Timmerman et al., 2004).

We thus attempted to examine the expression of a target gene in a context in which it is known to be strictly regulated by Notch signaling. During somitogenesis, *Lfng* exhibits dynamic oscillatory expression in the posterior presomitic mesoderm (PSM) under the control of Notch signaling (Cole et al., 2002; del Barco Barrantes et al., 1999; Morales et al., 2002; Morimoto et al., 2005). In the anterior PSM, it is stably expressed in stripe(s) under the control of the Mesp2 transcription factor (Morimoto et al., 2005), which is upregulated in part by Notch signaling (del Barco Barrantes et al., 1999). As shown in Fig. 7B-D, the double heterozygotes, or either of the single-null mutants at 9.0 dpc exhibited domains of *Lfng* expression in one of the three phases of the dynamic oscillatory expression in the posterior PSM (brackets) (Pourquie and Tam, 2001) and in stripes in the anterior PSM (arrowheads). By contrast, such a domain of *Lfng* expression in the posterior PSM (Fig. 7E, brackets) could not be detected, and the intensity of the stripe of *Lfng* expression was reduced in the anterior PSM (Fig. 7E, arrowheads)

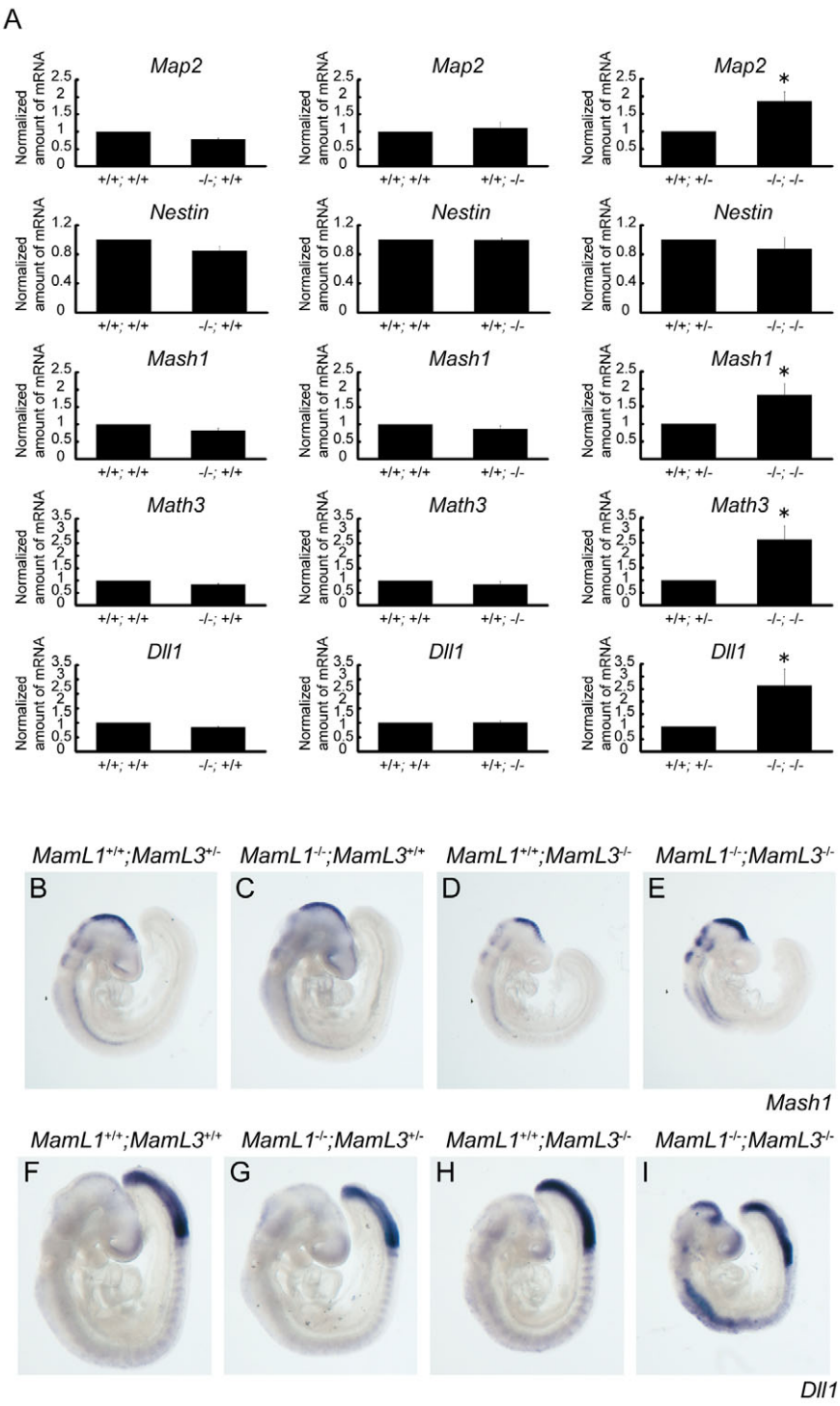

Fig. 6. Accelerated neurogenesis in *MamL1*$^{-/-}$;*MamL3*$^{-/-}$ double-null mutant mice. (**A**) Expression of mRNAs for five neural markers in total RNA isolated from single or double-null mutants and their littermate embryos at 9.5 dpc as assessed by real-time PCR (left column: MamL1-null mutants and their littermates; middle column: MamL3-null mutants and their littermates; right column: double-null mutants and their littermates). Each of the data represents the average of the three independent pairs performed in triplicate. The *y*-axis represents the mean value normalized to the level in the control embryos. Error bars indicate s.d. (n=3). *P<0.005 by Student's t-test. (**B-E**) Whole-mount in situ hybridization for *Mash1* in embryos at 8.5 dpc. The genotypes of each embryo are indicated. (**F-I**) Whole-mount in situ hybridization for *Dll1* in embryos at 9.5 dpc. The genotypes of each embryo are indicated.

of the double-null embryos (n=5). Expression of *Lfng* in nervous tissue, which has been shown to be independent of Notch signaling (Cole et al., 2002), was detected in the embryos irrespective of the genotype (Fig. 7B-E). These results are consistent with the notion that Notch signaling, in terms of target gene induction, was lost in the doubly null mice at least in this tissue.

Examination of the total RNA isolated from the embryos also revealed that the expression of *MamL1* or *MamL3* was disrupted in accordance with the genotypes (supplementary material Fig. S3). Interestingly, *MamL2* was expressed in all the mutants at similar levels (supplementary material Fig. S3).

Notch active transcriptional complex involving MamL2 is less stable than the complexes involving MamL1 or MamL3 in a computer-assisted simulation

The genetic analyses indicated that deletion of the two Mam family members resulted in a profound loss of Notch signaling during the organogenic period, even in the presence of the other family member, MamL2. When we compared the primary structures of the basic domains of the three Mam proteins, we found that the portion that would associate with the ankyrin domain of Notch (the Notch-binding domain) was well conserved among the three Mam

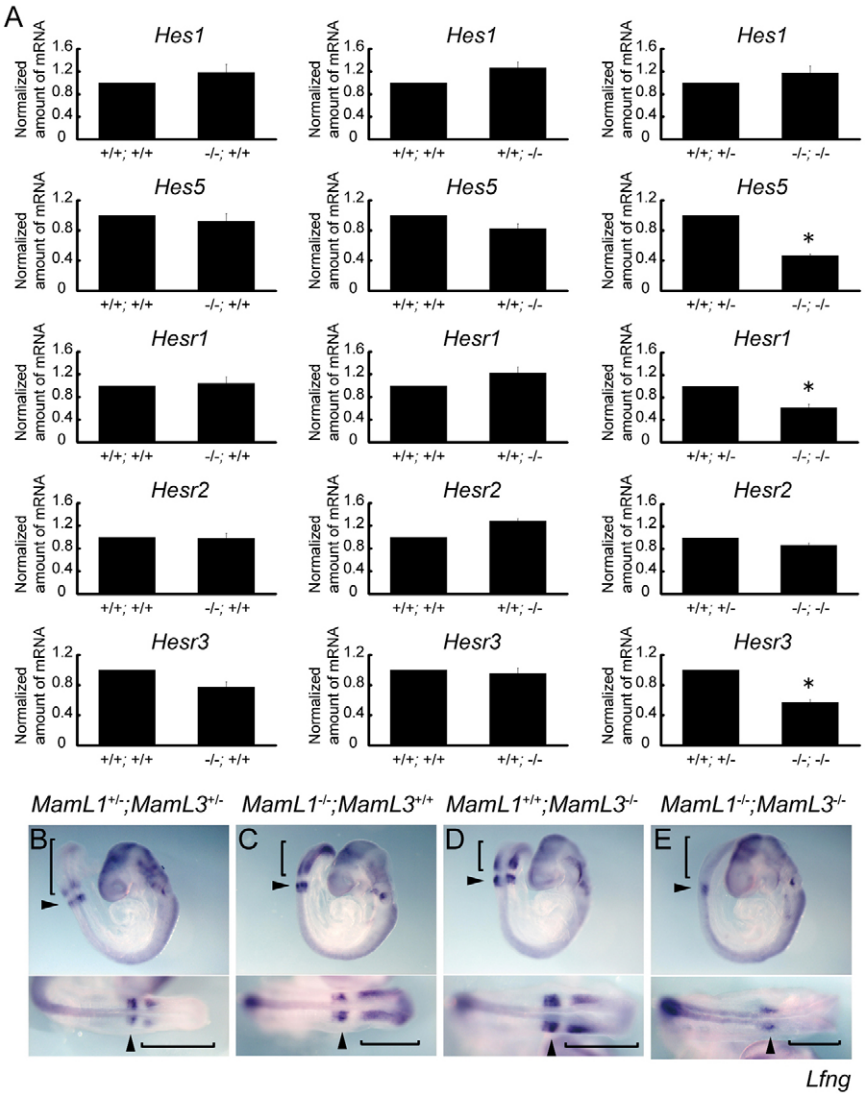

Fig. 7. Reduced expression of Notch target genes in *MamL1*$^{-/-}$;*MamL3*$^{-/-}$ double-null mutant mice. (**A**) Expression of mRNAs for five target genes of Notch signaling in total RNA isolated from single- or the double-null mutants and their littermate embryos at 9.5 dpc as assessed by real-time PCR (left column: MamL1-null mutants and their littermates; middle column: MamL3-null mutants and their littermates; right column: double-null mutants and their littermates). Each of the data represents the average of the three independent pairs performed in triplicate. The *y*-axis represents the mean value normalized to the level in the control embryos. Error bars indicate s.d. (n=3). *P<0.005 by Student's *t*-test. (**B-E**) Whole-mount in situ hybridization for *Lfng* in embryos (upper panels, lateral views; lower panels, dorsal views) at 9.0 dpc. The genotypes of each embryo are indicated. Brackets show the posterior PSM. Arrowheads show the anterior PSM.

proteins, whereas the portion of MamL2 that would associate with RBP-J (the RBP-J-binding domain) was relatively divergent compared with that of MamL1 and MamL3 (Fig. 8A). This prompted us to perform computer-assisted simulations to calculate the stability of complexes containing any of the three Mam sequences. Based on the published structure of the Mam-Notch-RBP-J-DNA complex, composed of portions of human MAML1, human NOTCH1 and human RBP-J (Nam et al., 2006), we first calculated structures for complexes containing any of the three murine Mams, murine Notch1, murine RBP-J and DNA by replacing the human homologs or paralogs in the original structure. The three structures were similar, as shown in Fig. 8B, which is their superimposed image. However, the time-dependent behavior of each of these structures computed by an MD simulation indicated that the RBP-J-binding domain and the hinge region (represented as a ribbon) of MamL2 were gradually expelled from the structure, whereas the equivalent portions of MamL1 or MamL3 were not (supplementary material Movie 1). Figure 8C shows the interaction energy between either of the portions of the three Mam proteins and RBP-J during this period. Electrostatic complementarities between the domains of MamL2 and RBP-J were markedly lower compared with those between the domains of the other two Mams and RBP-J (Table 2). These in silico analyses indicated that the complex involving MamL2 is less stable than those involving MamL1 or MamL3 and might explain our in vivo observations that MamL2 apparently cannot support Notch signaling in certain conditions.

Relative abundance of MamL1 and MamL3 correlates with their relative importance in vivo

An interesting point raised by the genetic analyses was that the relative importance of MamL1 and MamL3 changes during development. During midgestation, MamL1 and MamL3 play equivalent roles: the singly deficient mice showed none of the pan-Notch phenotypes whereas the doubly deficient mice exhibited all the phenotypes. By contrast, the role of MamL1 dominates that of MamL3 in the development of MZB cells after birth (Fig. 3) (Oyama et al., 2007). MamL1 also plays a more important role than MamL3 in the activation of a target promoter in primary cultured EFs (isolated from 14.5 dpc embryos) after ectopic expression of the intracellular domains of Notch (Fig. 2) (Oyama et al., 2007). To investigate the cause of these differences, we compared the expression levels of the endogenous MamL1 and MamL3 proteins in these tissues and cells by western blotting, using recombinant murine MamL1 and MamL3 proteins fused with a common epitope tag as controls. These analyses indicated that the expression of

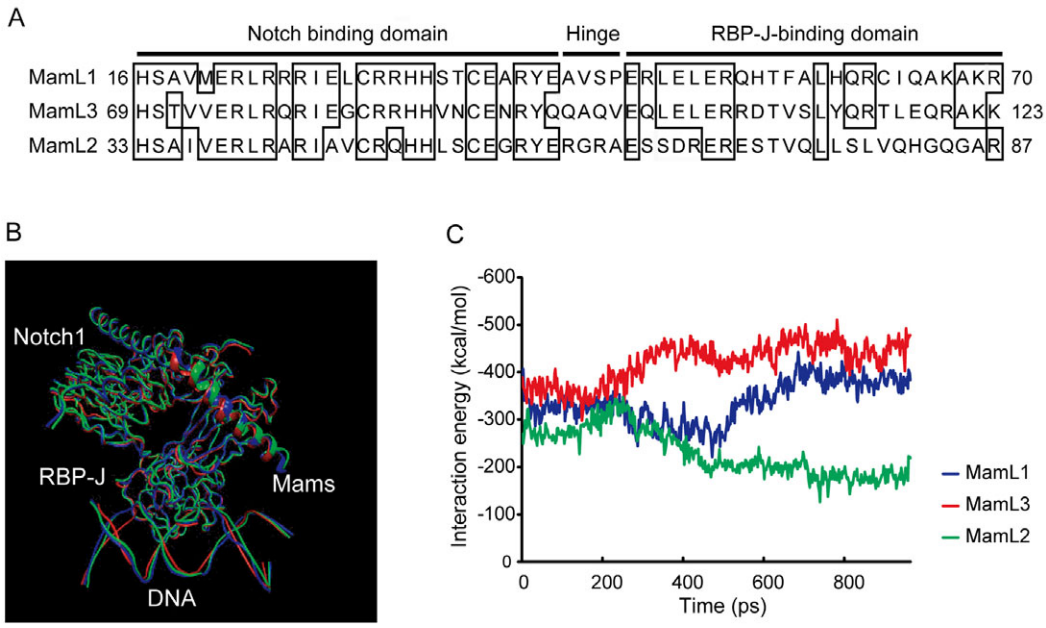

Fig. 8. Lower stability of the Mam-Notch-RBP-J-DNA complex involving MamL2. (**A**) Sequence alignment of the basic domains of the three murine Mams. The sequence of murine MamL2 was based on the sequence of the GenBank entry M_001013813.3. Boxed areas show identical amino acids. (**B**) Superimposed image of the structures of the Mam-Notch-RBP-J-DNA complexes constructed by replacing human MAML1, human NOTCH1 and human RBP-J in the original structure (Nam et al., 2006) with one of the three murine Mams, murine Notch1, and murine RBP-J. The structures involving MamL1, MamL3, and MamL2 are depicted in blue, red and green, respectively. (**C**) Trajectory of interaction energies for the hinge region and the RBP-J-binding domain of Mam and RBP-J calculated by MD simulation as shown in Movie 1 in the supplementary material. ps, picoseconds.

MamL1 and MamL3 in extracts from embryos at both 9.5 and 10.5 dpc was similar and within a threefold difference (Fig. 9A, legend). Both in the extract from splenic B lymphocytes isolated from 8-week-old mice and in that from EFs, the amount of MamL3 was small and was three to nine times smaller than the amount of MamL1 (Fig. 9B,C).

Figure 9D shows a re-examination of the extracts on a single blot. Based on the results shown in Fig. 9A, images were exposed to provide similar signals for MamL1 and MamL3 from the embryo extracts. In agreement with the results shown in Fig. 9A-C, the expression of MamL1 was only slightly reduced in the EFs and the splenic B cells compared with that in the embryos. Again confirming the titration assay, the expression of MamL3 was markedly reduced in the fibroblasts and the B cells. Overall, the relative expression levels of MamL1 and MamL3 correlated with the importance of these proteins in biological processes. Because in the crystal structures, the components of the Mam-Notch-RBP-J-DNA complex are in 1:1:1:1 stoichiometry, and the stability of the complexes involving MamL1 and MamL3 are similar (Fig. 8C, Table 2), the relative expression of the two proteins might explain their relative importance in vivo.

Interestingly, when we stripped the filter and blotted it with an anti-MamL2 antibody, we found that the expression of MamL2 in the fibroblasts and the B cells was significantly higher than that in the embryos (Fig. 9D). Unfortunately, however, as no full-length cDNA for *MamL2* is available at this moment, we could not titrate the blots for MamL2 relative to those for MamL1 and MamL3.

DISCUSSION

The classic pan-Notch phenotypes displayed by the *MamL1*$^{-/-}$;*MamL3*$^{-/-}$ mice indicate that Mam is necessary for Notch signaling in mammals. Altered expression of several Notch target genes in the embryos, especially loss of the *Lfng*-expressing domain in the posterior PSM, is consistent with this. Unexpectedly, the pan-Notch phenotypes were evident after disruption of just two of the three Mam genes.

Table 2. The maximum and minimum values of the interaction energies after the Mam-Notch-RBP-J-DNA complexes became stabilized (650 picoseconds) during the simulation shown in supplementary material Movie 1 and Fig. 8C

Interaction	Min or max	Time (ps)	Interaction energy (kcal/mol)	Electrostatic complementarity
MamL1-RBP-J	min	684	–442.4	0.77
	max	832	–338.1	0.65
MamL3-RBP-J	min	780	–509.4	0.74
	max	812	–394.4	0.68
MamL2-RBP-J	min	696	–232.0	0.49
	max	738	–126.6	0.27

max, maximum; min, minimum; ps, picoseconds.

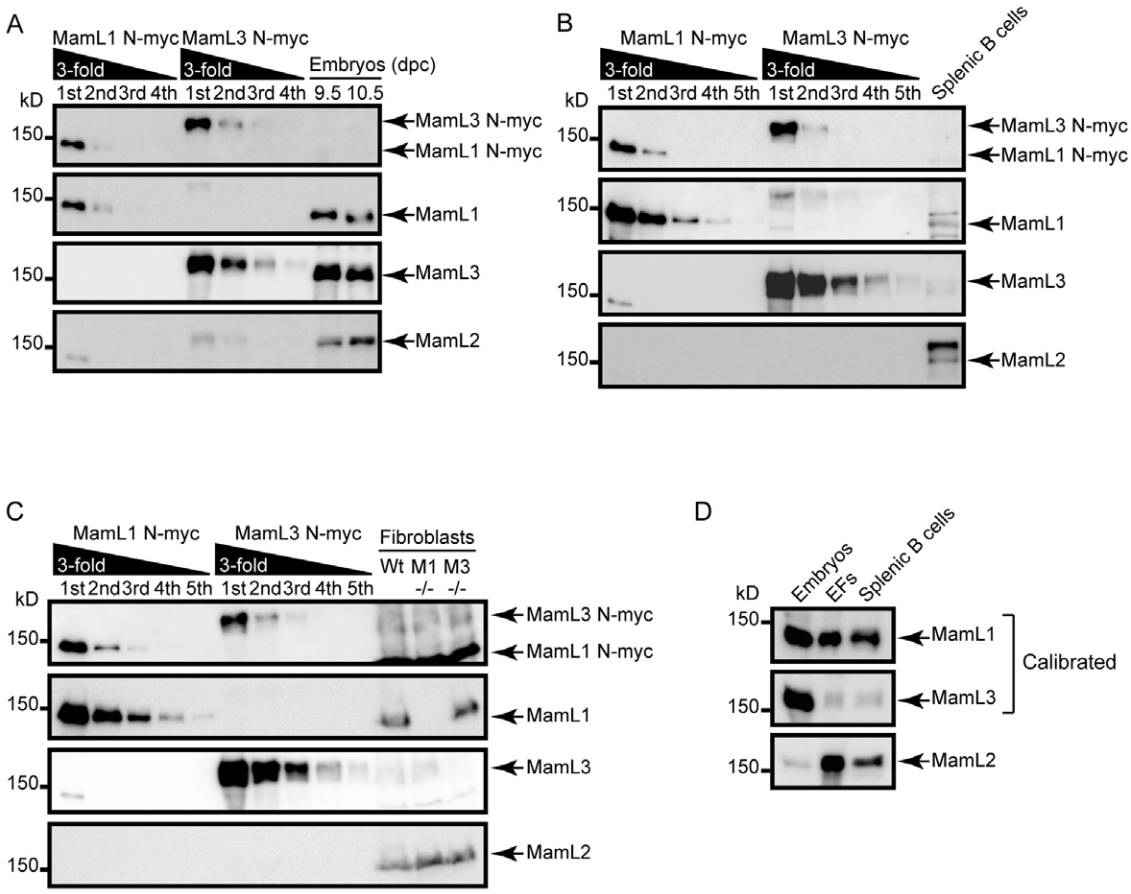

Fig. 9. Correlation of the relative amounts of Mam proteins and their in vivo importance. (**A**) Relative amounts of the Mam proteins in embryos at midgestation. Whole-cell extracts were prepared from C57BL/6 embryos at 9.5 or 10.5 dpc. The expression vectors for the murine MamL1 or MamL3 proteins tagged N-terminally with Myc epitope (MamL1 N-myc or MamL3 N-myc) were transfected into 293T cells. The extracts from these cells were loaded in threefold serial dilutions as indicated to provide similar signals on the anti-Myc tag blot for the tagged proteins as standards for quantification. Consecutive blotting with anti-Myc tag, anti-MamL1 and anti-MamL3 antibodies revealed that the amount of MamL1 in the extracts of embryos was in between that of the second and the third standards and that the amount of MamL3 was similar to that of the second standard. In addition, MamL2 was also expressed in these embryos. (**B**) Relative amounts of Mam proteins in splenic B cells. The amount of MamL1 in the extract was in between that of the third and the fourth standards. The amount of MamL3 in the extract was equivalent to that of the fifth standard. MamL2 was also expressed in these cells. (**C**) Relative amounts of Mam proteins in EFs. The amount of MamL1 was in between that of the third and the fourth standards. The amount of MamL3 was equivalent to that of the fifth standard. Wt, wild type; M1, MamL1; M3, MamL3. (**D**) Comparison of the expression of the three Mam proteins in C57BL/6 embryos at 10.5 dpc, EFs and splenic B cells. Based on the results in A, images were exposed to provide similar signals for MamL1 and MamL3 in the embryos. The image for MamL2 was exposed arbitrarily.

According to the MD simulation, MamL2, of which the primary structure is the most divergent among the Mam family, forms a complex that is less stable than those formed by MamL1 or MamL3. This might explain why Notch signaling is profoundly disrupted in the doubly deficient mice, even in the presence of MamL2. In the in vitro assays, the three Mam proteins showed similar functions (Lin et al., 2002). This might be because transfected Mam proteins would be expressed at much higher levels than the endogenous proteins and they could saturate even weak binding sites. Another possible explanation is that the expression of MamL2 in the embryos is low and is insufficient to support signaling strong enough to evoke biological responses. The relatively low expression of MamL2 in the embryos compared with the fibroblasts and the splenic B cells (Fig. 9D) hints at this. These two explanations are not mutually exclusive and might apply simultaneously.

Although the *Lfng*-expressing domain was undetectable in the posterior PSM of the *MamL1*$^{-/-}$*;MamL3*$^{-/-}$ embryos, the degree of reduction in *Hes5* expression in the mutants (Fig. 7A) appears to be more modest compared with that in the RBP-J mutants (de la Pompa et al., 1997). There is thus a possibility that the residual MamL2 still contributes to such remaining signaling activity, of which the strength seems insufficient to suppress the Notch phenotypes in some tissues.

The pan-Notch phenotypes seen in the *MamL1*$^{-/-}$*;MamL3*$^{-/-}$ mice have been shown to be dependent on Notch1 and Notch4 (Krebs et al., 2000), or Notch1 (de la Pompa et al., 1997). Thus, both MamL1 and MamL3 are likely to be able to participate in the ternary complexes in vivo that contain either of these Notch species. Although in the current study we could not examine phenotypes dependent on Notch2 or Notch3 in the double-null embryos because of their early death, we and others have already shown that MamL1 is necessary for Notch2-dependent development of splenic MZB cells (Oyama et al., 2007; Wu et al., 2007). Thus, MamL1 can form part of the in vivo ternary complex containing at least Notch1, Notch2 and Notch4. These results are consistent with the results of the luciferase assay,

which showed that MamL1 deficiency affects signaling by all four Notch proteins (Fig. 2B). They are also consistent with our previous results involving overexpression of these components (Lin et al., 2002). However, as the degree of reduction of the activation evoked by the four NotchICs in the MamL1-deficient fibroblasts is variable (20-50% of the wild-type cells, depending on the type of NotchIC), subtle preferences between Mam and Notch species might exist.

Recombinant Notch1IC and RBP-J proteins form complexes in vitro in the absence of Mam (Ishitani et al., 2010; Nam et al., 2003). In the Mam-NotchIC-RBP-J transcription-activating complex, a major activation domain is provided by Notch (Kurooka and Honjo, 2000; Oyama et al., 2007). Thus, one may envisage that the Notch-RBP-J complex can activate the target genes to a greater or lesser extent to induce its biological consequences. However, the genetic evidence obtained here clearly shows that the activity provided by the Notch-RBP-J complex is insufficient to evoke such outcomes. Mam is indispensable for activating the complex sufficiently to execute biological responses, possibly, at least in part, by stabilizing the complex.

Consistent with the studies involving overexpression (Lin et al., 2002), the gene dosage of MamL1 correlates well with the strength of Notch signaling, especially for Notch2, Notch3 and Notch4 (Fig. 2B). Furthermore, the gene dosage also correlates with a particular phenotype, the generation of splenic MZB cells (Wu et al., 2007). Thus, Mam potentially serves as a regulatory point for the signaling strength, and its modification might have biological significance.

The results shown in Fig. 9D might be consistent with the notion that MamL2 plays a role in supporting Notch signaling later in life than 10.5 dpc. Indeed, it has recently been shown that aberrantly expressed MAML2 in human lymphomas contributes to pathological activation of Notch signaling in these cells (Köchert et al., 2011). Thus, MamL2 might be the factor that supports the residual signaling activity seen in the MamL1-deficient fibroblasts (Fig. 2B). Further work, such as analysis of mice mutant for *MamL2*, is necessary to clarify these issues.

In contrast to MamL1, single deficiency of MamL3 results in a benign phenotype. However, we have shown that MamL3 plays a redundant role with MamL1 to support Notch signaling during the early organogenic period. Thus, it is possible that MamL3 also plays a similar redundant role in later development, although the lethality of the double-deficient mice hampered such analysis in the current study.

Overall, each of the three mammalian Mam species seems to have a unique role in vivo. This is reminiscent of the case for the four mammalian Notch species (Conlon et al., 1995; Domenga et al., 2004; Hamada et al., 1999; Kitamoto and Hanaoka, 2010; Krebs et al., 2000; Radtke et al., 2010; Swiatek et al., 1994). However, assignment of roles to the Notch species seems to have occurred independently from that of the Mam species. Thus, different combinations of Mam-Notch might have distinct in vivo functions, depending on spatiotemporal criteria.

Acknowledgements
We thank T. Honjo, S. Chiba, L. Strobl, T. Sudo, R. Kageyama, S. Seino and S. Nagata for reagents used in this study; and A. Sakamoto, T. Tokuhisa, S. Hirahara, M. Yamashita, T. Nakayama, Y.-Y. Kong, Y. Muroyama, T. Saito, Y. Shida, A. Toyoda, H. Kawana, M. Higashi, K. Azuma and T. Umemiya for help.

Funding
This work was supported by Grants-in-Aid for Scientific Research from the Ministry of Education, Culture, Sports, Science and Technology of Japan [18590257, 18012011].

Competing interests statement
The authors declare no competing financial interests.

Supplementary material
Supplementary material available online at
http://dev.biologists.org/lookup/suppl/doi:10.1242/dev.062802/-/DC1

References
Alves-Guerra, M. C., Ronchini, C. and Capobianco, A. J. (2007). Mastermind-like 1 Is a specific coactivator of beta-catenin transcription activation and is essential for colon carcinoma cell survival. *Cancer Res.* **67**, 8690-8698.
Artavanis-Tsakonas, S., Matsuno, K. and Fortini, M. E. (1995). Notch signaling. *Science* **268**, 225-232.
Barsi, J. C., Rajendra, R., Wu, J. I. and Artzt, K. (2005). Mind bomb1 is a ubiquitin ligase essential for mouse embryonic development and Notch signaling. *Mech. Dev.* **122**, 1106-1117.
Bozkulak, E. C. and Weinmaster, G. (2009). Selective use of ADAM10 and ADAM17 in activation of Notch1 signaling. *Mol. Cell. Biol.* **29**, 5679-5695.
Bray, S. J. (2006). Notch signalling: a simple pathway becomes complex. *Nat. Rev. Mol. Cell Biol.* **7**, 678-689.
Chen, H., Ko, G., Zatti, A., Di Giacomo, G., Liu, L., Raiteri, E., Perucco, E., Collesi, C., Min, W., Zeiss, C. et al. (2009). Embryonic arrest at midgestation and disruption of Notch signaling produced by the absence of both epsin 1 and epsin 2 in mice. *Proc. Natl. Acad. Sci. USA* **106**, 13838-13843.
Cole, S. E., Levorse, J. M., Tilghman, S. M. and Vogt, T. F. (2002). Clock regulatory elements control cyclic expression of Lunatic fringe during somitogenesis. *Dev. Cell* **3**, 75-84.
Conlon, R. A., Reaume, A. G. and Rossant, J. (1995). Notch1 is required for the coordinate segmentation of somites. *Development* **121**, 1533-1545.
de la Pompa, J. L., Wakeham, A., Correia, K. M., Samper, E., Brown, S., Aguilera, R. J., Nakano, T., Honjo, T., Mak, T. W., Rossant, J. et al. (1997). Conservation of the Notch signalling pathway in mammalian neurogenesis. *Development* **124**, 1139-1148.
del Barco Barrantes, I., Elia, A. J., Wunsch, K., Hrabe de Angelis, M. H., Mak, T. W., Rossant, J., Conlon, R. A., Gossler, A. and de la Pompa, J. L. (1999). Interaction between Notch signalling and Lunatic fringe during somite boundary formation in the mouse. *Curr. Biol.* **9**, 470-480.
Dequeant, M. L. and Pourquie, O. (2008). Segmental patterning of the vertebrate embryonic axis. *Nat. Rev. Genet.* **9**, 370-382.
Domenga, V., Fardoux, P., Lacombe, P., Monet, M., Maciazek, J., Krebs, L. T., Klonjkowski, B., Berrou, E., Mericskay, M., Li, Z. et al. (2004). Notch3 is required for arterial identity and maturation of vascular smooth muscle cells. *Genes Dev.* **18**, 2730-2735.
Donoviel, D. B., Hadjantonakis, A. K., Ikeda, M., Zheng, H., Hyslop, P. S. and Bernstein, A. (1999). Mice lacking both presenilin genes exhibit early embryonic patterning defects. *Genes Dev.* **13**, 2801-2810.
Evrard, Y. A., Lun, Y., Aulehla, A., Gan, L. and Johnson, R. L. (1998). lunatic fringe is an essential mediator of somite segmentation and patterning. *Nature* **394**, 377-381.
Greenwald, I. (2005). LIN-12/Notch signaling in *C. elegans*. In *WormBook* (ed. The *C. elegans* Research Community), doi/10.1895/wormbook.1.10.1, http://www.wormbook.org.
Hamada, Y., Kadokawa, Y., Okabe, M., Ikawa, M., Coleman, J. R. and Tsujimoto, Y. (1999). Mutation in ankyrin repeats of the mouse Notch2 gene induces early embryonic lethality. *Development* **126**, 3415-3424.
Hartmann, D., de Strooper, B., Serneels, L., Craessaerts, K., Herreman, A., Annaert, W., Umans, L., Lubke, T., Lena Illert, A., von Figura, K. et al. (2002). The disintegrin/metalloprotease ADAM 10 is essential for Notch signalling but not for alpha-secretase activity in fibroblasts. *Hum. Mol. Genet.* **11**, 2615-2624.
Hatakeyama, J., Bessho, Y., Katoh, K., Ookawara, S., Fujioka, M., Guillemot, F. and Kageyama, R. (2004). Hes genes regulate size, shape and histogenesis of the nervous system by control of the timing of neural stem cell differentiation. *Development* **131**, 5539-5550.
Herreman, A., Hartmann, D., Annaert, W., Saftig, P., Craessaerts, K., Serneels, L., Umans, L., Schrijvers, V., Checler, F., Vanderstichele, H. et al. (1999). Presenilin 2 deficiency causes a mild pulmonary phenotype and no changes in amyloid precursor protein processing but enhances the embryonic lethal phenotype of presenilin 1 deficiency. *Proc. Natl. Acad. Sci. USA* **96**, 11872-11877.
Hrabe de Angelis, M., McIntyre, J., 2nd and Gossler, A. (1997). Maintenance of somite borders in mice requires the Delta homologue Dll1. *Nature* **386**, 717-721.
Ishitani, T., Hirao, T., Suzuki, M., Isoda, M., Ishitani, S., Harigaya, K., Kitagawa, M., Matsumoto, K. and Itoh, M. (2010). Nemo-like kinase suppresses Notch signalling by interfering with formation of the Notch active transcriptional complex. *Nat. Cell Biol.* **12**, 278-285.
Itoh, F., Itoh, S., Goumans, M. J., Valdimarsdottir, G., Iso, T., Dotto, G. P., Hamamori, Y., Kedes, L., Kato, M. and ten Dijke, P. (2004). Synergy and

antagonism between Notch and BMP receptor signaling pathways in endothelial cells. *EMBO J.* **23**, 541-551.
Jin, B., Shen, H., Lin, S., Li, J. L., Chen, Z., Griffin, J. D. and Wu, L. (2010). The mastermind-like 1 (MAML1) co-activator regulates constitutive NF-kappaB signaling and cell survival. *J. Biol. Chem.* **285**, 14356-14365.
Kageyama, R., Ohtsuka, T., Shimojo, H. and Imayoshi, I. (2008). Dynamic Notch signaling in neural progenitor cells and a revised view of lateral inhibition. *Nat. Neurosci.* **11**, 1247-1251.
Kitagawa, M., Oyama, T., Kawashima, T., Yedvobnick, B., Kumar, A., Matsuno, K. and Harigaya, K. (2001). A human protein with sequence similarity to Drosophila mastermind coordinates the nuclear form of notch and a CSL protein to build a transcriptional activator complex on target promoters. *Mol. Cell. Biol.* **21**, 4337-4346.
Kitamoto, T. and Hanaoka, K. (2010). Notch3 null mutation in mice causes muscle hyperplasia by repetitive muscle regeneration. *Stem Cells* **28**, 2205-2216.
Köchert, K., Ullrich, K., Kreher, S., Aster, J. C., Kitagawa, M., Jöhrens, K., Anagnostopoulos, I., Jundt, F., Lamprecht, B., Zimber-Strobl, U. et al. (2011). High-level expression of Mastermind-like 2 contributes to aberrant activation of the NOTCH signaling pathway in human lymphomas. *Oncogene* **30**, 1831-1840.
Koo, B. K., Lim, H. S., Song, R., Yoon, M. J., Yoon, K. J., Moon, J. S., Kim, Y. W., Kwon, M. C., Yoo, K. W., Kong, M. P. et al. (2005). Mind bomb 1 is essential for generating functional Notch ligands to activate Notch. *Development* **132**, 3459-3470.
Kopan, R. and Ilagan, M. X. (2009). The canonical Notch signaling pathway: unfolding the activation mechanism. *Cell* **137**, 216-233.
Krebs, L. T., Xue, Y., Norton, C. R., Shutter, J. R., Maguire, M., Sundberg, J. P., Gallahan, D., Closson, V., Kitajewski, J., Callahan, R. et al. (2000). Notch signaling is essential for vascular morphogenesis in mice. *Genes Dev.* **14**, 1343-1352.
Kurooka, H. and Honjo, T. (2000). Functional interaction between the mouse notch1 intracellular region and histone acetyltransferases PCAF and GCN5. *J. Biol. Chem.* **275**, 17211-17220.
Li, T., Ma, G., Cai, H., Price, D. L. and Wong, P. C. (2003). Nicastrin is required for assembly of presenilin/gamma-secretase complexes to mediate Notch signaling and for processing and trafficking of beta-amyloid precursor protein in mammals. *J. Neurosci.* **23**, 3272-3277.
Lin, S. E., Oyama, T., Nagase, T., Harigaya, K. and Kitagawa, M. (2002). Identification of new human mastermind proteins defines a family that consists of positive regulators for notch signaling. *J. Biol. Chem.* **277**, 50612-50620.
Lindberg, M. J., Popko-Scibor, A. E., Hansson, M. L. and Wallberg, A. E. (2010). SUMO modification regulates the transcriptional activity of MAML1. *FASEB J.* **24**, 2396-2404.
Mansouri, A., Yokota, Y., Wehr, R., Copeland, N. G., Jenkins, N. A. and Gruss, P. (1997). Paired-related murine homeobox gene expressed in the developing sclerotome, kidney, and nervous system. *Dev. Dyn.* **210**, 53-65.
Minoguchi, S., Taniguchi, Y., Kato, H., Okazaki, T., Strobl, L. J., Zimber-Strobl, U., Bornkamm, G. W. and Honjo, T. (1997). RBP-L, a transcription factor related to RBP-Jkappa. *Mol. Cell. Biol.* **17**, 2679-2687.
Mizushima, S. and Nagata, S. (1990). pEF-BOS, a powerful mammalian expression vector. *Nucleic Acids Res.* **18**, 5322.
Moellering, R. E., Cornejo, M., Davis, T. N., Del Bianco, C., Aster, J. C., Blacklow, S. C., Kung, A. L., Gilliland, D. G., Verdine, G. L. and Bradner, J. E. (2009). Direct inhibition of the NOTCH transcription factor complex. *Nature* **462**, 182-188.
Morales, A. V., Yasuda, Y. and Ish-Horowicz, D. (2002). Periodic Lunatic fringe expression is controlled during segmentation by a cyclic transcriptional enhancer responsive to notch signaling. *Dev. Cell* **3**, 63-74.
Morimoto, M., Takahashi, Y., Endo, M. and Saga, Y. (2005). The Mesp2 transcription factor establishes segmental borders by suppressing Notch activity. *Nature* **435**, 354-359.
Nakashima, K., Takizawa, T., Ochiai, W., Yanagisawa, M., Hisatsune, T., Nakafuku, M., Miyazono, K., Kishimoto, T., Kageyama, R. and Taga, T. (2001). BMP2-mediated alteration in the developmental pathway of fetal mouse brain cells from neurogenesis to astrocytogenesis. *Proc. Natl. Acad. Sci. USA* **98**, 5868-5873.
Nam, Y., Weng, A. P., Aster, J. C. and Blacklow, S. C. (2003). Structural requirements for assembly of the CSL.intracellular Notch1.Mastermind-like 1 transcriptional activation complex. *J. Biol. Chem.* **278**, 21232-21239.
Nam, Y., Sliz, P., Song, L., Aster, J. C. and Blacklow, S. C. (2006). Structural basis for cooperativity in recruitment of MAML coactivators to Notch transcription complexes. *Cell* **124**, 973-983.
Nishimura, M., Yokoi, N., Miki, T., Horikawa, Y., Yoshioka, H., Takeda, J., Ohara, O. and Seino, S. (2004). Construction of a multi-functional cDNA library specific for mouse pancreatic islets and its application to microarray. *DNA Res.* **11**, 315-323.
Oka, C., Nakano, T., Wakeham, A., de la Pompa, J. L., Mori, C., Sakai, T., Okazaki, S., Kawaichi, M., Shiota, K., Mak, T. W. et al. (1995). Disruption of the mouse RBP-J kappa gene results in early embryonic death. *Development* **121**, 3291-3301.
Okazaki, N., Kikuno, R., Ohara, R., Inamoto, S., Koseki, H., Hiraoka, S., Saga, Y., Nagase, T., Ohara, O. and Koga, H. (2003). Prediction of the coding sequences of mouse homologues of KIAA gene: III. the complete nucleotide sequences of 500 mouse KIAA-homologous cDNAs identified by screening of terminal sequences of cDNA clones randomly sampled from size-fractionated libraries. *DNA Res.* **10**, 167-180.
Oyama, T., Harigaya, K., Muradil, A., Hozumi, K., Habu, S., Oguro, H., Iwama, A., Matsuno, K., Sakamoto, R., Sato, M. et al. (2007). Mastermind-1 is required for Notch signal-dependent steps in lymphocyte development in vivo. *Proc. Natl. Acad. Sci. USA* **104**, 9764-9769.
Pourquie, O. and Tam, P. P. (2001). A nomenclature for prospective somites and phases of cyclic gene expression in the presomitic mesoderm. *Dev. Cell* **1**, 619-620.
Radtke, F., Fasnacht, N. and Macdonald, H. R. (2010). Notch signaling in the immune system. *Immunity* **32**, 14-27.
Roca, C. and Adams, R. H. (2007). Regulation of vascular morphogenesis by Notch signaling. *Genes Dev.* **21**, 2511-2524.
Saga, Y., Hata, N., Kobayashi, S., Magnuson, T., Seldin, M. F. and Taketo, M. M. (1996). MesP1: a novel basic helix-loop-helix protein expressed in the nascent mesodermal cells during mouse gastrulation. *Development* **122**, 2769-2778.
Sakano, D., Kato, A., Parikh, N., McKnight, K., Terry, D., Stefanovic, B. and Kato, Y. (2010). BCL6 canalizes Notch-dependent transcription, excluding Mastermind-like1 from selected target genes during left-right patterning. *Dev. Cell* **18**, 450-462.
Sanalkumar, R., Dhanesh, S. B. and James, J. (2010). Non-canonical activation of Notch signaling/target genes in vertebrates. *Cell. Mol. Life Sci.* **67**, 2957-2968.
Sasaki, N., Kiso, M., Kitagawa, M. and Saga, Y. (2011). The repression of Notch signaling occurs via the destabilization of mastermind-like 1 by Mesp2 and is essential for somitogenesis. *Development* **138**, 55-64.
Serneels, L., Dejaegere, T., Craessaerts, K., Horre, K., Jorissen, E., Tousseyn, T., Hebert, S., Coolen, M., Martens, G., Zwijsen, A. et al. (2005). Differential contribution of the three Aph1 genes to gamma-secretase activity in vivo. *Proc. Natl. Acad. Sci. USA* **102**, 1719-1724.
Shen, H., McElhinny, A. S., Cao, Y., Gao, P., Liu, J., Bronson, R., Griffin, J. D. and Wu, L. (2006). The Notch coactivator, MAML1, functions as a novel coactivator for MEF2C-mediated transcription and is required for normal myogenesis. *Genes Dev.* **20**, 675-688.
Shi, S. and Stanley, P. (2003). Protein O-fucosyltransferase 1 is an essential component of Notch signaling pathways. *Proc. Natl. Acad. Sci. USA* **100**, 5234-5239.
Swiatek, P. J., Lindsell, C. E., del Amo, F. F., Weinmaster, G. and Gridley, T. (1994). Notch1 is essential for postimplantation development in mice. *Genes Dev.* **8**, 707-719.
Timmerman, L. A., Grego-Bessa, J., Raya, A., Bertran, E., Perez-Pomares, J. M., Diez, J., Aranda, S., Palomo, S., McCormick, F., Izpisua-Belmonte, J. C. et al. (2004). Notch promotes epithelial-mesenchymal transition during cardiac development and oncogenic transformation. *Genes Dev.* **18**, 99-115.
Tonooka, A., Kubo, T., Ichimiya, S., Tamura, Y., Ilmarinen, T., Ulmanen, I., Kimura, S., Yokoyama, S., Takano, Y., Kikuchi, T. et al. (2009). Wild-type AIRE cooperates with p63 in HLA class II expression of medullary thymic stromal cells. *Biochem. Biophys. Res. Commun.* **379**, 765-770.
van Tetering, G., van Diest, P., Verlaan, I., van der Wall, E., Kopan, R. and Vooijs, M. (2009). Metalloprotease ADAM10 is required for Notch1 site 2 cleavage. *J. Biol. Chem.* **284**, 31018-31027.
Wilson, J. J. and Kovall, R. A. (2006). Crystal structure of the CSL-Notch-Mastermind ternary complex bound to DNA. *Cell* **124**, 985-996.
Wu, L., Aster, J. C., Blacklow, S. C., Lake, R., Artavanis-Tsakonas, S. and Griffin, J. D. (2000). MAML1, a human homologue of Drosophila mastermind, is a transcriptional co-activator for NOTCH receptors. *Nat. Genet.* **26**, 484-489.
Wu, L., Sun, T., Kobayashi, K., Gao, P. and Griffin, J. D. (2002). Identification of a family of mastermind-like transcriptional coactivators for mammalian notch receptors. *Mol. Cell. Biol.* **22**, 7688-7700.
Wu, L., Maillard, I., Nakamura, M., Pear, W. S. and Griffin, J. D. (2007). The transcriptional coactivator Maml1 is required for Notch2-mediated marginal zone B-cell development. *Blood* **110**, 3618-3623.
Zhao, Y., Katzman, R. B., Delmolino, L. M., Bhat, I., Zhang, Y., Gurumurthy, C. B., Germaniuk-Kurowska, A., Reddi, H. V., Solomon, A., Zeng, M. S. et al. (2007). The notch regulator MAML1 interacts with p53 and functions as a coactivator. *J. Biol. Chem.* **282**, 11969-11981.